J Fluoresc (2015) 25:1469–1480
DOI 10.1007/s10895-015-1638-6

ORIGINAL ARTICLE

Rigid Coumarins: a Complete DFT, TD-DFT and Non Linear Optical Property Study

Sandip K. Lanke[1] · **Nagaiyan Sekar**[1]

Received: 25 April 2015 / Accepted: 3 August 2015 / Published online: 13 August 2015

Abstract The electronic structures and photophysical properties of rigid coumarin dyes have been studied by using quantum chemical methods. The ground-state geometries of these dyes were optimized using the Density Functional Theory (DFT) methods. The lowest singlet excited state was optimized using Time -Dependent Density Functional Theory [TD-B3LYP/6-31G(d)]. On the basis of ground- and excited-state geometries, the absorption and emission spectra have been calculated using the DFT and TD-DFT method. All the calculations were carried out in gas phase and in acetonitrile medium. The results show that the absorption maxima and fluorescence emission maxima calculated using the Time-Dependent Density Functional Theory is in good agreement with the available experimental results. To understand the Non- Linear Optical properties of coumarin dyes we computed dipole moment (μ), electronic polarizability (α), mean first hyperpolarizability (βo) and second hyperpolarizability (γ) using B3LYP density functional theory method in conjunction with 6-31G(d) basis set.

Keywords Rigid coumarins · DFT · TD-DFT · Hyperpolarizability study

Electronic supplementary material The online version of this article (doi:10.1007/s10895-015-1638-6) contains supplementary material, which is available to authorized users.

✉ Nagaiyan Sekar
n.sekar@ictmumbai.edu.in; nethi.sekar@gmail.com

[1] Tinctorial Chemistry Group, Department of Dyestuff Technology, Institute of Chemical Technology, (Formerly UDCT), Nathalal Parekh Marg, Matunga, Mumbai 400 019, India

Introduction

Coumarins are found to be attractive fluorophores as they possess promising photophysical properties like intense fluorescence, high quantum yields (up to 0.99) [1, 2], high molar extinction coefficients (10,000–54,300) [1, 3] and large Stokes shifts (up to 160 nm) [4]. Coumarin dyes show high degree of sensitivity in terms of their photophysical properties to their local environment [5]. They show very good solvotochromic properties and hence they have been extensively employed in membrane-staining agents, since they localize preferentially on cell membrane, where the fluorescence is enhanced [6]. These attractive photophysical properties promoted their use as functional dyes; coumarins are thoroughly investigated as a fluorescent probes for living cell imaging [7–9]. Coumarins are the most widely used fluorophores for developing highly selective and sensitive fluorescent probes for metal anions and cations [10–12], they are also used in dye lasers for the blue and green regions [13, 14]. Compared to the metal-complex sensitizers, metal-free coumarin dyes adopting the donor-π-acceptor structure motif are under wide investigation due to their high molar extinction coefficients, simple and easy preparation processes promoted their use in dye sensitized solar cells (DSSC's) [15, 16]. Coumarin derivatives are widely used in organic light emitting diodes (OLEDs) due to its high triplet energy and high hole transporting ability [17, 18].

Moreover, it is possible to tune their optoelectronic properties through minor structural modification by changing substitution pattern like introduction of electron releasing group at the 7 position of chromone ring like *N,N*-diethyl amine, diphenyl amine, methoxy, hydroxyl, carbazole, julolidine [19–22] etc. This substitution pattern not only increases the emission properties but also alters the optical and electro-optical properties like large dipole moment, high molar

extinction coefficient, high stokes shift. Syzova et al. reported bichromophoric fluorescent coumarin dyes with rigid molecular structure; these compounds are very sensitive to solvent polarity and pH [1]. These coumarin dyes not only show high quantum yield but also high molar extinction coefficient. They investigated the absorption and emission spectra of these compounds in acetonitrile solution and reported their absorption and emission spectra. Their results show that the absorption and emission spectra are in the UV-to-visible region.

To understand the experimentally observed photophysical properties of these compounds with a view to design new rigid coumarin dyes with the desirable properties, theoretical investigations on the structure property relationship of these materials are essential. Quantum mechanical investigation plays an important role to investigate the relationship between electronic structures and the photophysical (both linear and nonlinear optical) properties of the organic molecules [23–25]. The main aim of the present work is to investigate the ground- and excited-state optimized geometries, polarizabilities and hyperpolarizabilities arising out of ground and excited state geometries, and the optical absorption and emission properties of rigid coumarins, and their various substitution pattern using DFT and TD-DFT.

The structures of the various rigid coumarin molecules studied are shown in Fig. 1. The structure optimization at the excited-state is much more challenging job than the optimization at the ground-state. This is because the excited states are often more diffused and basis sets lacking the analytical derivatives of the energy with respect to atomic displacements: that is, forces on atoms cannot be calculated directly. In addition, the information that can be extracted from experiment about the excited state geometry is very limited. The wave function-based electron correlation methods such as configuration interaction singles (CIS), complete active space perturbation theory (CASPT2), configuration interaction singles–second-order Møller-Plesset perturbation theory (CIS-MP2) and symmetry adapted cluster/configuration interaction (SAC-CI) are the best choices to calculate the excited-state geometry and optoelectronic properties. Because CIS method have some good features like (a) it is comparatively faster than the other methods, (b) it is very easy to set up the number of excited electronic state and basis set, and (c) it is possible to discuss the electronic transitions such as π-π^*. From the properties one can compare bond length and bond angle differences between ground and excited states. But main drawback with CIS method is that it gives accurate excitation energies only for electronic transitions that are influenced by single excitations. Otherwise, there is common error of 1 eV, which makes it difficult to assign observed spectral lines in the absence of symmetry. For low-lying electronic states time-dependent density functional theory (TD-DFT) is useful [26].

In the recent years, the extension of density functional theory (DFT) to the time dependent domain, namely time-dependent density functional theory (TD-DFT) has become a powerful tool for the calculation of the energies, structures, and properties of electronically excited states (ES) of organic molecules; their computational cost still prevents application to variety of systems of photochemical interest. Thus, there is a considerable interest in extending the capabilities of TD-DFT to even larger molecules, beyond hundreds of atoms in the molecule. There are number reports available in the literature, where computational results are comparable with the experimental results [27, 28]. TD-DFT method has emerged as a standard method to study the photophysical properties like vertical transition energies, determination of ES structures, emission wavelengths, the estimation of atomic point charges, dipole moments and the computation of vibrationally resolved optical spectra, as well as the simulation of photochemical reactions [24].

In the present study, we therefore focus considerable attention on the application of DFT and TD-DFT to the rigid coumarins because this type of coumarin fluorophores show intense fluorescence with quantum yield close to unity. In this paper, hybrid functional B3LYP was employed both in the density functional theory (DFT) calculation for the ground state and TD-DFT calculation for the excited state for the various rigid coumarins. On the basis of these optimized geometries we have calculated the absorption and emission spectra using the TD-DFT method with the B3LYP exchange correlation functional using 6-31G(d) basis set. In this work we have also computed dipole moment (μ), electronic polarizability (α), mean first hyperpolarizability (βo) and second order hyperpolarizability (γ).

Theory/Computational Method

The molecular geometries have been optimized using the Gaussian 09 suite of programs [29]. The ground state (S_0) geometry of the coumarin dyes were optimized in the gas phase as well as in acetonitrile medium using DFT [30]. The functional used was B3LYP. The B3LYP method combines Becke's three parameter exchange functional (B3) [31] with the nonlocal correlation functional by Lee, Yang and Parr (LYP) [32]. The basis set used for all atoms was 6- 31G (d). The vibrational frequencies at the optimized structures were computed using the same method to verify that the optimized structures correspond to local minima on the energy surface. The vertical excitation energies and oscillator strengths were obtained for the lowest ten singlet-singlet transitions at the optimized the ground state equilibrium geometries by using the Time Dependent Density Functional Theory (TD-DFT) at the same hybrid functional and basis set [26, 33, 34]. Frequency calculations are carried out to ensure that each

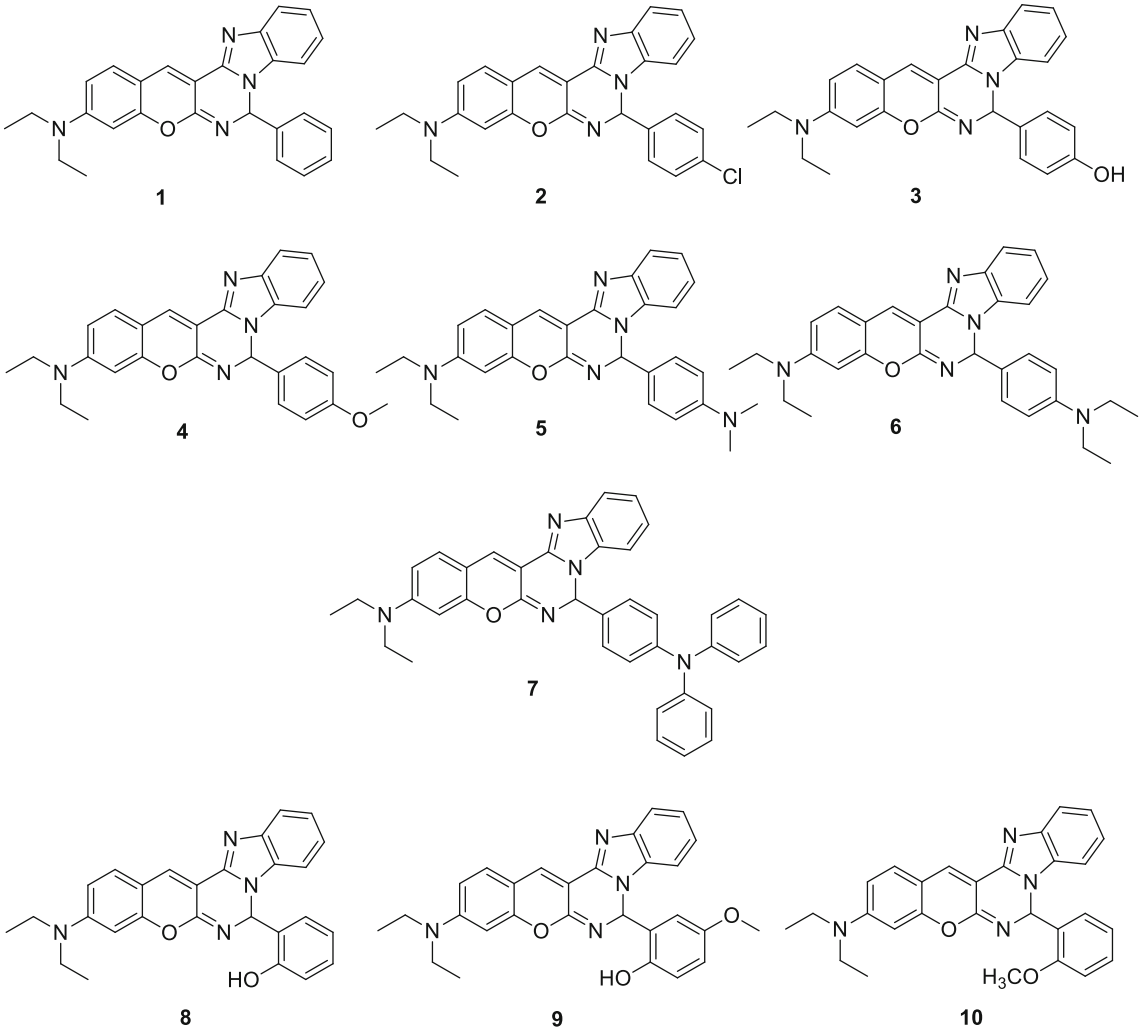

Fig. 1 Structure of coumarins

optimized conformation has all positive frequencies and thus is a minimum on the potential energy surface. The low-lying first singlet excited states (S1) of the dyes were relaxed using the TD-DFT to obtain their minimum energy geometries. We have done TD-DFT of the optimized first singlet excited state geometries for calculating the emission [35]. Frequency computations were also carried out on the excited state geometry of the dyes. All the computations were carried out initially in gas phase and in acetonitrile solvent using the Self-Consistent Reaction Field (SCRF) under the Polarizable Continuum Model (PCM) [36, 37]. The electronic absorption spectra, including absorption wavelengths, oscillators strengths, and main configuration assignment, were systematically investigated using TD-DFT with PCM model on the basis of the optimized ground structures

In this work we have also calculated dipole moment (μ), electronic polarizability (α), mean first hyperpolarizability (β_0) and second hyperpolarizability (γ) using B3LYP functional with the 6-31G(d) basis set. For completeness, we will here briefly summarize the essential formulas used in our work, highlighting the quantities in which we are interested.

Here, second-order NLO properties of the rigid coumarin chromophore **1**–**10** with donor N,N-diethyl coumarin core and acceptor benzimidazole core were calculated by using density functional theory (DFT). Although accurate values for the hyperpolarizabilities of coumarin molecules of this size are difficult to calculate but in this paper we have done an attempt to understand the nonlinear optical response of these type of coumarin derivatives. The coumarins are somewhat more complicated structures to calculate these properties. The static first hyperpolarizability (βo) and second hyperpolarizability (γ) and its related properties for coumarin dyes **1**–**10** (Fig. 1) were calculated using B3LYP/6-31G(d) on the basis of the finite field approach [38, 39]. In the presence of an applied field, the energy of the system is a function of the electric field,

and the first hyperpolarizability is a third rank tensor that can be described by a 3×3×3 matrix. The 27 components of the 3D matrix can be reduced to ten components because of the Kleinman symmetry [40]. The matrix can be given in the lower tetrahedral format. It is obvious that the lower part of the 3×3×3 matrix is a tetrahedral. The components of β are defined as the co-efficient in the Taylor series expansion of the energy in the external electric field. When the external electric field is weak and homogeneous, this expansion becomes.

$$E = E^{\circ} - \mu_{\alpha} f_{\alpha} - \frac{1}{2\alpha_{\alpha\beta} F_{\alpha} F_{\beta}} - \frac{1}{6\beta_{\alpha\beta\gamma} F_{\alpha} F_{\beta} F_{\gamma}} \cdots \quad (1)$$

Where E° is the energy of the unperturbed molecules, F_{α} is the field at the origin, μ_{α}, $\alpha_{\alpha\beta}$ and $\beta_{\alpha\beta\gamma}$ are the components of dipole moment, polarizability and the first hyperpolarizabilities, respectively.

The total static dipole moment μ is expressed by following equation

$$\mu = \sqrt{\mu_x^2 + \mu_y^2 + \mu_z^2} \quad (2)$$

The isotropic polarizability can be calculated from the trace of the polarization tensor,

$$\alpha_0 = \frac{(\alpha_{xx} + \alpha_{yy} + \alpha_{zz})}{3} \quad (3)$$

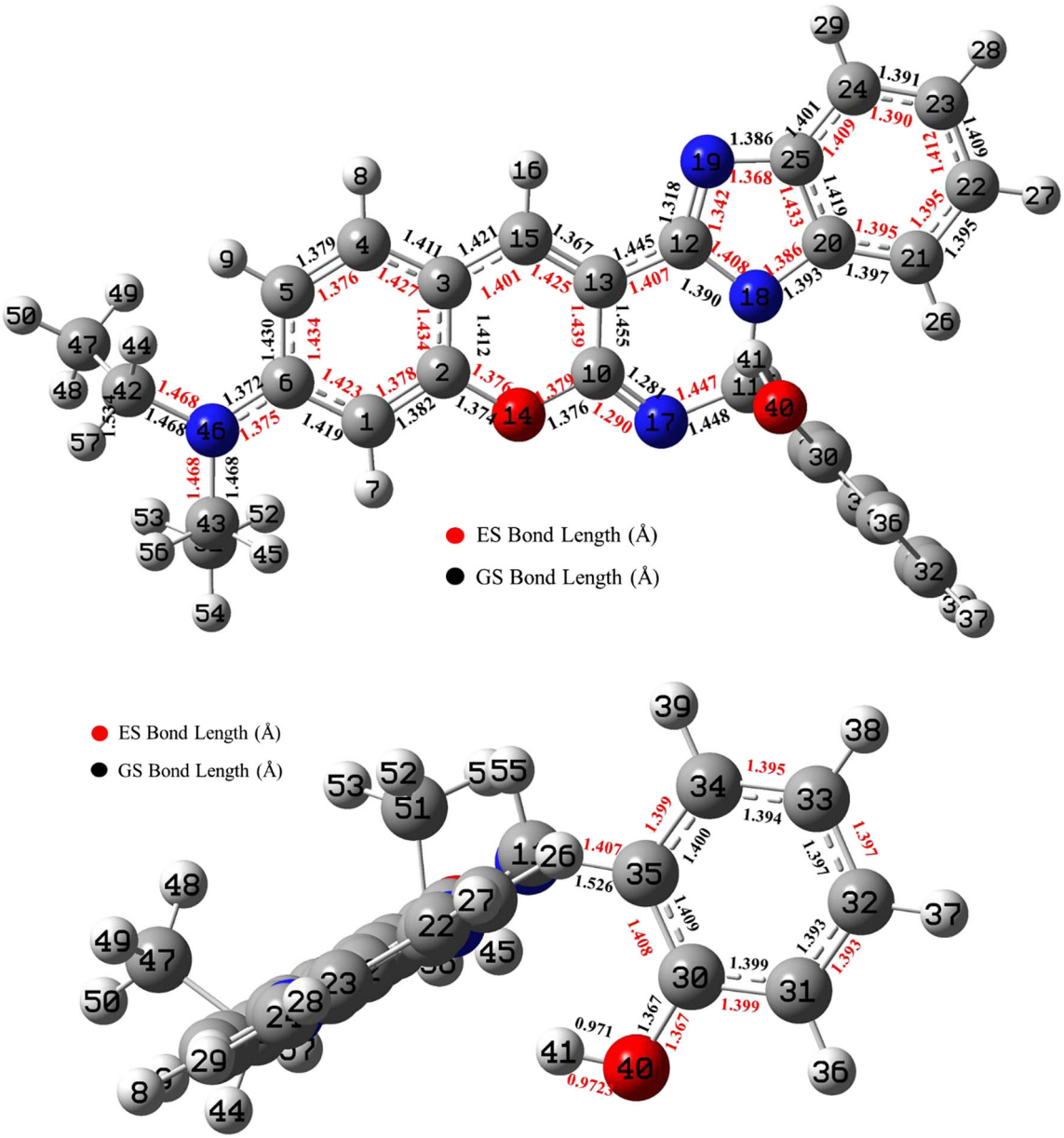

Fig. 2 Optimized geometry parameters of coumarin dye 8 in acetonitrile solvent in the ground state (GS) and excited state (ES) (Front and side view)

Table 1 Computed vertical transitions and their orbital contributions along with the oscillator strength of various coumarin derivatives at the B3LYP/6-31G(d) level

Dye	[a] λ_{max}^{abs} nm	TD-DFT						%D ACN
		Absorption energy				[b]*f* acetonitrile	CI coefficients of major excitations (Acetonitrile)	
		(λ) eV acetonitrile	Gas	nm Acetonitrile	Gas			
1	436	2.9435	3.0833	421	402	1.2442	HOMO→LUMO (98 %)	3.4
2	437	2.9563	3.0946	419	400	1.2282	HOMO→LUMO (98 %)	4.1
3	437	2.9602	3.0987	418	400	1.2125	HOMO→LUMO (98 %)	4.3
4	436	2.9425	3.1016	421	399	1.2453	HOMO→LUMO (98 %)	3.4
5	436	2.8747	3.0185	431	410	0.6264	HOMO→LUMO (72 %)	1.1
		3.0218	3.1809	410	389	0.6295	HOMO-1→LUMO (72 %)	5.9
6	437	2.8973	3.0125	427	411	0.6169	HOMO→LUMO (72 %)	2.2
		3.0351	3.1715	408	390	0.6255	HOMO-1→LUMO (72 %)	6.6
7	436	2.7732	2.8014	447	442	0.0434	HOMO→LUMO (98 %)	2.5
8	434	2.9117	3.0688	425	404	1.2537	HOMO→LUMO (98 %)	2.0
9	–	3.1226	3.0688	397	404	0.6911	HOMO-1→LUMO (74 %)	–
10	433	3.1052	3.1637	399	391	1.0306	HOMO→LUMO (98 %)	7.9

[a] absorption maxima value taken from ref [1], [b] *f*=oscillator strength

Anisotropy of the polarizability $\Delta\alpha$ is expressed by

$$\Delta\alpha = 2^{-1/2}\left[\left(\alpha_{xx}+\alpha_{yy}\right)^2+\left(a_{zz}+\alpha_{xx}\right)^2+6\alpha_{xx}^2\right] \quad (4)$$

The mean first polarizability (β_0) is expressed by

$$\beta_0 = \left(\beta_x^2+\beta_y^2+\beta_z^2\right)^{1/2} \quad (5)$$

$$\beta_0 = \left[\left(\beta_{xxx}+\beta_{xyy}+\beta_{xzz}\right)^2+\left(\beta_{yxx}+\beta_{yyy}+\beta_{yzz}\right)^2+\left(\beta_{zxx}+\beta_{zyy}+\beta_{zzz}\right)^2\right]^{\frac{1}{2}} \quad (6)$$

Where, β_x, β_y, and β_z are the components of the second-order polarizability tensor along the x, y, and z axes

The mean second hyperpolarazibility (γ) is expressed by

$$\gamma = \frac{1}{6}\left[\left(\gamma_{xxxx}+\gamma_{yyyy}+\gamma_{zzzz}\right)+2\left(\gamma_{xxxx}+\gamma_{yyyy}+\gamma_{zzzz}\right)\right] \quad (7)$$

Results and Discussion

Geometric Structures in the Ground State

To understand the ground-state geometry of coumarin dyes with different substitution pattern have been optimized at B3LYP/6-31G(d) level of theory using C_1 point group. As shown in the Fig. 2 the bond length N_{46}-C_6 is increased from 1.372 to 1.375 Å. While the bond length C_5-C_4 is shortened. The lengths of bridged bonds (i.e., the carbon–carbon single bond between two consecutive oligomers) for the C_{12}-C_{13} for coumarin **1**–**10** are within 1.429–1.439 Å, in the ground state and 1.445–1.461 Å in the excited state which are ~0.1 Å shorter than that of ethane (1.54 Å)(See Table S1). This is due to the partial double-bond character on the bridge bond between the chromone ring and the imidazole unit caused by π-bonding interaction, thereby strengthening and shortening the bridge bond. While the bond length C_{12}-N_{19} for coumarin **1**–**10** are within 1.318–1.324 Å, in the S_0 state and 1.342–1.347 Å in the S_1 state (See Table S2), which indicates that the double bond character of C-N are reduced to the single bond. This change in the bond length indicates that there is charge transfer observed from *N,N*-diethyl amino group to imidazole group. There are no significant changes observed for other bond length like C_{21}-C_{22}, C_{24}-C_{23}. The benzene ring which is perpendicular to the chromone show no change in the bond length. The dihedral angle N_{18}-C_{10}-C_{23}-C_{22}, for

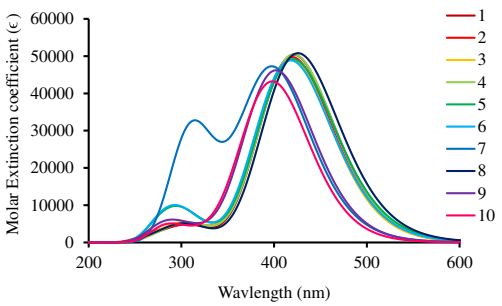

Fig. 3 The absorption spectra of coumarins 1–10 computed at TD-B3LYP/6-31G(d) level of theory in acetonitrile medium

Table 2 Electronic distribution in the frontier molecular orbitals of the coumarin derivatives 1–10 calculated at B3LYP/6-31G(d) level of theory in acetonitrile medium

Dye	HOMO-1	HOMO	LUMO	LUMO+1
1	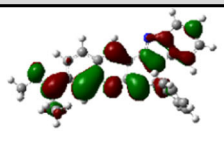	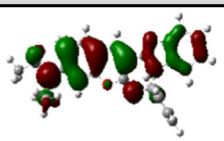	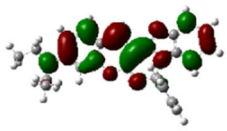	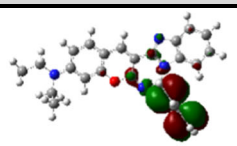
2	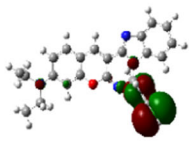	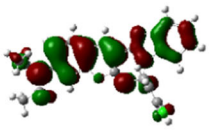	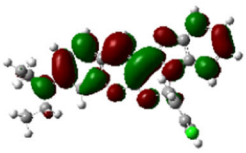	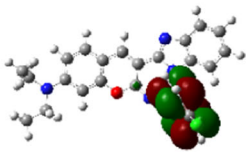
3	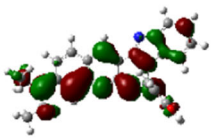	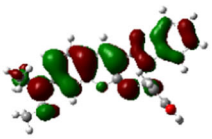	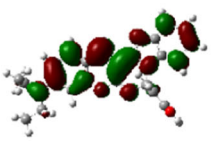	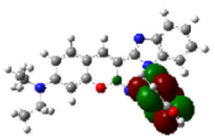
4	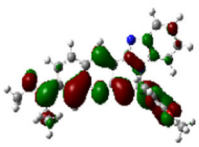	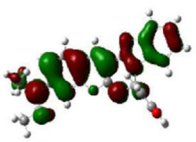	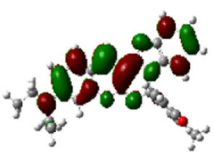	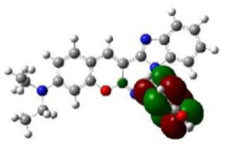
5	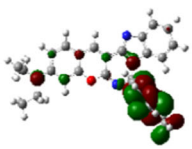	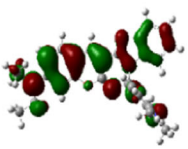	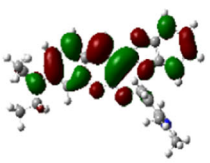	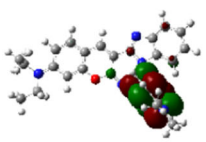
6	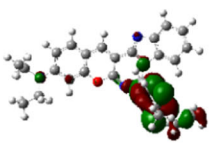	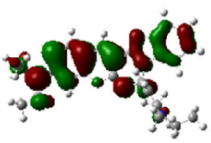	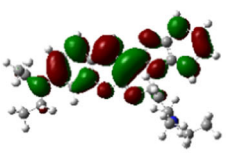	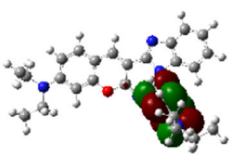
7	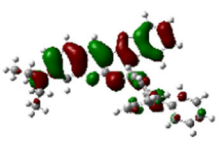	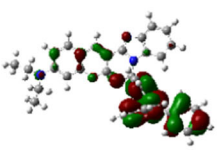	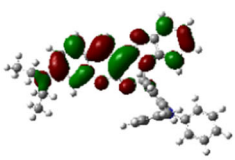	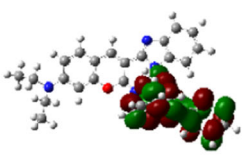
8	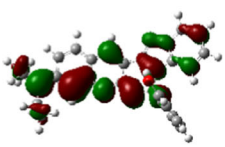	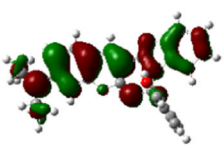	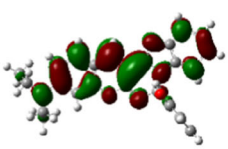	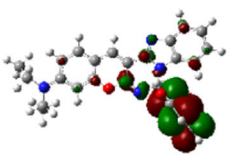
9	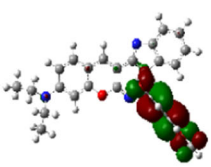	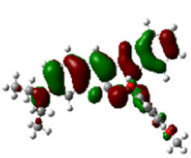	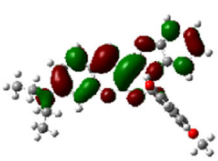	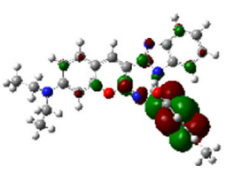

coumarin **10** in acetonitrile solvent in S_0 state is 66.7° while in S_1 state it is 66.3° while for coumarin **5** it is 56.7° in S_0 state and 30.9° in S_1 state which indicates that the phenyl ring connected with chromone moiety and imidazole segment does not affect more change in coumarin **10** but it changes in coumarin **5** indicating that due to ortho methoxy group the phenyl ring is more perpendicular to the chromone moity as compared to p-n,n-dimethyl amine group.

Electronic Vertical Excitation Spectra

The computed vertical excitation spectra associated with their oscillator strengths, composition, and assignments of the chromophores as well as the corresponding experimental

λ_{max} of the respective coumarin dyes **1**–**10** in acetonitrile solvent is shown in Table 1. All the dyes with various substitution patterns do not affect the absorption wavelength. The theoretical λ_{max} reported in the following corresponds to the first singlet excited states with dipole allowed transition (i.e., oscillator strength *f* is >0) from the ground state. From the experimental observation it is noteworthy that all the dyes show absorption wavelength in the range of 433 to 437 nm. The absorption spectra for all the dyes are mainly due to the electronic transition from the highest occupied molecular orbital (HOMO) to the lowest unoccupied molecular orbital (LUMO). The major contribution seen for the dyes **2**, **3**, **8** and **10** is near about 98 % while for dyes **5**, **6** and **9** it is about 72–74 %. The calculated absorption wavelength for dye **5** is 431 nm for HOMO→LUMO transition and it is well accordance with corresponding experimental absorption peak is 436 nm with 1.1 % deviation. While in the case of other dyes such as the dye **3** the calculated absorption wavelength is 418 nm while that of experimental is 437 nm and the difference is 19 nm (4.3 % D). The largest difference of 34 nm (7.9 % D) is observed for the dye **10** and the lowest difference of 5 nm (1.1 % D) is observed for the dye **5**. The compound **7**

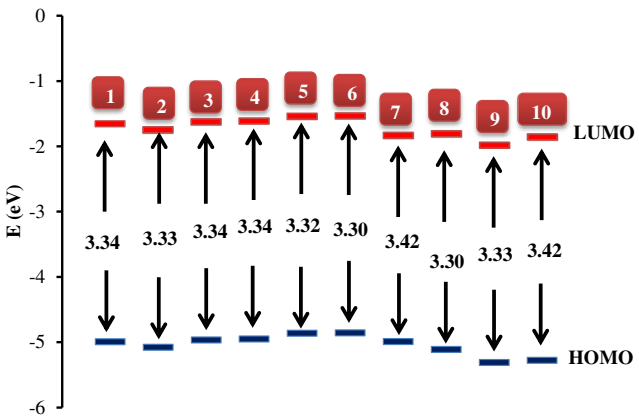

Fig. 4 Frontier Molecular Orbitals (FMOs) energy level diagram of dye 1–10 in gas phase

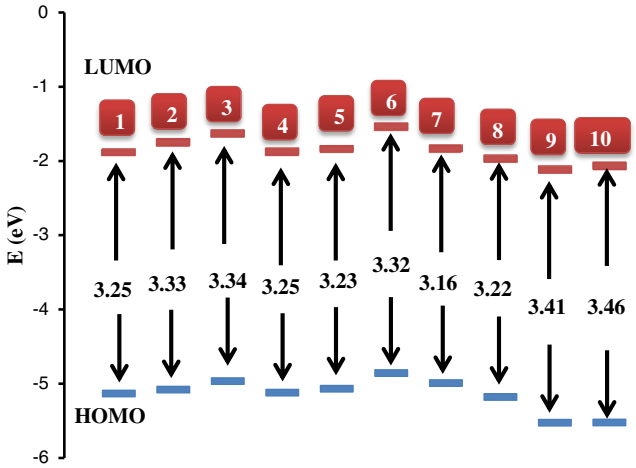

Fig. 5 Frontier Molecular Orbitals (FMOs) energy level diagram of dye 1–10 in acetonitrile solvent

shows absorption at 447 nm with very less oscillator strength 0.0434 but at higher oscillator strength (*f*=1.1276) the absorption peaks appear at 398 nm. The absorption spectra for the coumarins **1**–**10** in acetonitrile solvent computed at TD-B3LYP/6-31G(d) level of theory are shown in Fig. 3.

Molecular Orbital Energies

Energy levels of the frontier molecular orbitals especially HOMO, LUMO, HOMO-1 and LUMO+1 as well as their spatial distributions are crucial parameters for determining the optoelectronic properties. The density plot of the HOMO and LUMO of rigid coumarin derivatives **1**–**10** are calculated

Table 3 Energy of HOMO, LUMO, and band gaps of the coumarin dyes 1–10 in gas phase and acetonitrile using TDDFT (B3LYP/6-31G(d)) method

Dye	Gas			Acetonitrile		
	$^{a}E_{HOMO}$ (eV)	$^{b}E_{LUMO}$ (eV)	E_L-E_H	$^{a}E_{HOMO}$ (eV)	$^{b}E_{LUMO}$ (eV)	E_L-E_H
1	−4.9929	−1.6552	3.3377	−5.1301	−1.8797	3.2504
2	−5.0770	−1.7442	3.3328	−5.0770	−1.7442	3.3328
3	−4.9655	−1.6248	3.3407	−4.9655	−1.6248	3.3407
4	−4.9521	−1.6131	3.3390	−5.1203	−1.8691	3.2512
5	−4.8626	−1.5396	3.3230	−5.0659	−1.8376	3.2283
6	−4.8569	−1.5342	3.3227	−4.8569	−1.5342	3.3227
7	−4.9905	−1.8291	3.1614	−4.9905	−1.8291	3.1614
8	−5.1100	−1.8063	3.3037	−5.1774	−1.9622	3.2152
9	−5.3116	−1.9818	3.3298	−5.5257	−2.1113	3.4144
10	−5.2784	−1.8547	3.4237	−5.5206	−2.0607	3.4599

[a] Energy of highest occupied molecular orbital (HOMO). [b] Energy of lowest unoccupied molecular orbital (LUMO)

Table 4 Experimental UV-Visible emission and computed emission from TD-B3LYP/6-31G(d) computations for the coumarin dyes 1–10 in acetonitrile solvent

Compound No.	λ_{max}^{abs} (nm)	λ_{max}^{ems} [a] (nm)	λ_{max}^{abs} (cm^{-1})	λ_{max}^{ems} (cm^{-1})	$\Delta\overline{v}$ (cm^{-1})	Є ($lmol^{-1}$ cm^{-1})	σ (cm^2)	ϕ	TD-B3LYP/ 6-31G(d) λ_{max}^{ems} [b] (nm)	% D
01	436	498	22960	20080	2880	51200	195840	0.98	465	6.6
02	437	499	22900	20040	2260	–	–	0.97	465	6.8
03	437	498	22900	20080	2820	51200	195840	0.99	466	6.4
04	436	499	22940	20060	2880	50500	193163	0.96	466	6.6
05	436	499	22960	20040	2920	50500	193163	0.10	455	8.8
06	437	499	22900	20060	2280	51500	196988	0.03	454	9.0
07	436	499	22920	20040	2880	54300	207698	0.90	479	4.0
08	434	499	23040	20040	3000	44900	171743	0.97	467	6.4
09	–	–	–	–	–	–	–	–	468	
10	433	497	23080	20120	2960	47600	182070	0.98	466	6.2

All experimental values were taken from reference [1]. Here, λ_{max}^{abs} absorption maxima, λ_{max}^{ems} [a] emission maxima obtained experimentally, λ_{max}^{ems} [b] emission maxima obtained theoretically using B3LYP/6-31G(d), ε molar extinction at long-wavelength absorption maxima, $\Delta\overline{v}_{ST}$ Stokes shift, σ absorption area of cross section, ϕ fluorescence quantum yield. Extinction data for 05 is not available owing to its low solubility in acetonitrile

at B3LYP/6-31G(d) level of theory and are shown in Table 2. The orbital diagrams are plotted with the contour value of 0.025 a.u. The plots of the HOMO and LUMO of the studied coumarin molecules have the typical π molecular orbital characteristics and are slightly altered by the substitution. From the molecular orbital analysis, we infer that the lowest lying singlet-singlet absorption as well as emission corresponds to the electronic transition of π-π* type.

Table 2 illustrates that, for the coumarins, both HOMO and LUMO are fully delocalized over the entire coumarin core except the substituted phenyl ring containing various substituents. But it is noteworthy that the introduction of triphenyl amine core to coumarin **7** slightly alters the HOMO. The HOMO of **7** shows that the electron density is concentrate on the triphenyl moiety and not on the coumarin core while LUMO shows the usual behaviour. The energy of the frontier molecular orbitals of coumarin derivatives obtained at B3LYP/ 6-31G(d) level of theory in gas phase and acetonitrile medium are presented in Figs. 4 and 5 respectively. The HOMO (H)-LUMO (L) energy gap of coumarins **1**–**10** is found in the range of 3.16 to 3.42 eV in the gas phase and 3.16 to 3.45 eV in acetonitrile medium. The lowest energy gap is observed for coumarin **7**. For both coumarin **6** and **7** the HOMO energy is slightly increased upon the introduction of *N,N*-diethylaniline and triphenyl amine group. The HOMO-LUMO energy value are presented in Table 3.

Coumarin **1**–**10** were optimized in the first excited state to calculate the fluorescence. Experimentally obtained fluorescence emission spectral data and emission computed from TD-B3LYP/6-31G(d) computations are shown in Table 4. The experimental emission wavelength and emission computed by TD-B3LYP/6-31G(d) showed the largest difference of 44 nm in acetonitrile solvent for coumarin **6** and **7** however minimum difference of 32 nm for coumarin **3** and 33 nm for coumarin **1**. The emission spectra of coumarin **1**–**10** in acetonitrile solvent are shown in Fig. 6.

Nonlinear Optical (NLO) Properties

We have calculated the static dipole moment (μ), mean polarizability (α_0), polarizability anisotropy ($\Delta\alpha$), static first hyperpolarizability (β_0) and second hyperpolarizability (γ) at the ground and the excited state for ten coumarin molecules and which are gathered in Tables 5 and 6 respectively (More details are provided in supporting information, Table S3-SS13). As can be seen, the mean polarizabilities of all coumarin chromophores are almost the same in gas phase as well as in acetonitrile solvent. But in case of polarizability anisotropy ($\Delta\alpha$), coumarin **6** shows higher value (7117.68×10^{-24} esu) while that of coumarin **2** shows the lowest value of 5161.27×

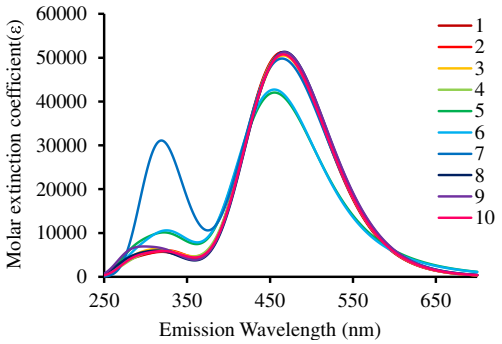

Fig. 6 The emission spectra of coumarins 1–10 computed at TD-B3LYP/6-31G(d) level of theory in acetonitrile medium

Table 5 Static dipole moment (μ), mean polarizability (α_0), polarizability anisotropy ($\Delta\alpha$), First hyperpolarizability (β_0) and second hyperpolarizability (γ) calculated at B3LYP level using 6-31G(d) basis set by GAUSSIAN 09 for all coumarin dyes at the ground state (1–10)

Dye	μ(au)		$\alpha_0\times10^{-24}$(esu)		$\Delta\alpha\times10^{-24}$(esu)		$\beta_0\times10^{-30}$(esu)		$\gamma\times10^{-36}$(esu)	
	Gas	ACN	Gas	ACN	Gas	ACN	Gas	ACN	Gas	ACN
1	2.50	3.33	56.67	76.88	5756.41	10698.88	27.23	119.97	195.36	687.22
2	2.67	3.42	58.61	78.78	5161.27	9472.38	34.43	122.45	203.34	702.98
3	2.22	2.90	57.29	77.20	6232.98	11428.35	27.62	115.75	200.91	697.12
4	2.18	3.04	59.44	80.37	6614.51	12361.97	27.28	116.72	206.23	703.63
5	2.38	3.35	62.26	84.30	6648.15	12838.75	24.90	111.49	218.25	735.16
6	2.16	2.83	65.80	87.81	7117.68	12541.52	26.77	111.81	222.40	747.19
7	1.57	2.05	77.51	102.5	7963.07	13362.51	13.96	43.30	264.78	768.20
8	2.50	3.51	57.48	78.51	5750.99	11232.48	35.85	134.34	195.17	682.81
9	1.36	1.28	57.60	77.92	5522.46	9910.03	11.94	57.83	193.97	607.60
10	1.42	1.88	58.05	77.15	5403.37	9693.01	15.68	21.60	199.98	598.41
Urea	–	–	3.830	–	2410.00	–	0.37	–	0.68	–

10^{-24} esu. Such a large value can be attributed to the lower compactness structure of this coumarin chromophore. It is well-known that second-order nonlinear optical (NLO) properties originate from the non-centrosymmetric alignment of NLO chromophores. Urea and p-nitroaniline (pNA) are prototypical compounds used in the study of the NLO properties of molecular systems. We have calculated first hyperpolarizability of these coumarin molecules at B3LYP/6-31G(d) level of theory. The computed values for the first hyperpolarizability (β_o) for the coumarins **1**–**10** were found to be greater than urea (3.71028×10^{-31}) by 73, 93, 74, 73, 67, 72, 37, 96, 32 and 42 times respectively using the B3LYP functional in the gas phase. In dichloromethane, the β_o values were found to be 324, 330, 312, 301, 302, 363 for coumarin **1**–**6** and **8** respectively however for coumarins **7**, **9** and **10** are found to be 117, 156 and 58 times greater compared to the gas phase. This obtained large β_o value confirmes that there should be charge transfer characterisics of the first excited state. This is might be due to the rigidity of coumarin which leads to large hyperpolarazibility. The low value of β_o for compound **7**, **9** and **10** suggest that due to ortho hydroxy and triphenyl amine group makes the phenyl ring slightly twist which disturbs the planarity of the chromone which leads to decrease in beta value. The experimentaly calculated values of β for urea and p-nitroaniline are 89.73 and 1287.09 au respectively. Static first hyperpolarizability of coumarin **8** is nearly 46 times greater than corresponding experimental values of urea, and three times higher than that of

Table 6 Static dipole moment (μ), mean polarizability (α_0), polarizability anisotropy ($\Delta\alpha$), First hyperpolarizability (β_0) and second hyperpolarizability (γ) calculated at B3LYP level using 6-31G(d) basis set by GAUSSIAN 09 for all coumarin dyes at the excited state (1–10)

Dye	μ(au)		$\alpha_0\times10^{-24}$(esu)		$\Delta\alpha\times10^{-24}$(esu)		$\beta_0\times10^{-30}$(esu)		$\gamma\times10^{-36}$(esu)	
	Gas	ACN	Gas	ACN	Gas	ACN	Gas	ACN	Gas	ACN
1	2.61	3.87	59.61	83.27	7111.18	15069.97	15.39	92.93	187.24	705.05
2	2.96	4.24	61.82	85.70	6662.48	14309.40	17.15	95.17	191.68	711.54
3	2.43	3.64	60.50	84.31	7358.57	15794.81	15.41	92.00	191.23	710.62
4	2.44	3.60	62.70	86.84	8168.45	16897.69	15.44	90.91	196.33	723.54
5	2.18	3.27	63.28	87.97	6373.73	13342.57	16.10	86.63	234.73	918.06
8	3.12	4.07	60.25	84.59	7700.11	15494.58	14.35	103.53	185.07	676.66
6	2.16	3.19	66.75	92.31	6161.48	13673.28	16.29	86.93	234.51	946.33
7	2.60	3.70	80.57	112.46	3945.99	18047.33	20.93	91.91	249.51	910.17
8	3.12	4.07	60.25	84.59	7700.11	15494.58	14.35	103.53	185.07	676.66
9	2.91	3.74	63.96	88.02	7098.06	15407.61	31.01	102.76	287.93	697.20
10	2.28	3.41	62.11	86.43	8360.29	17181.95	13.10	85.71	184.83	699.67

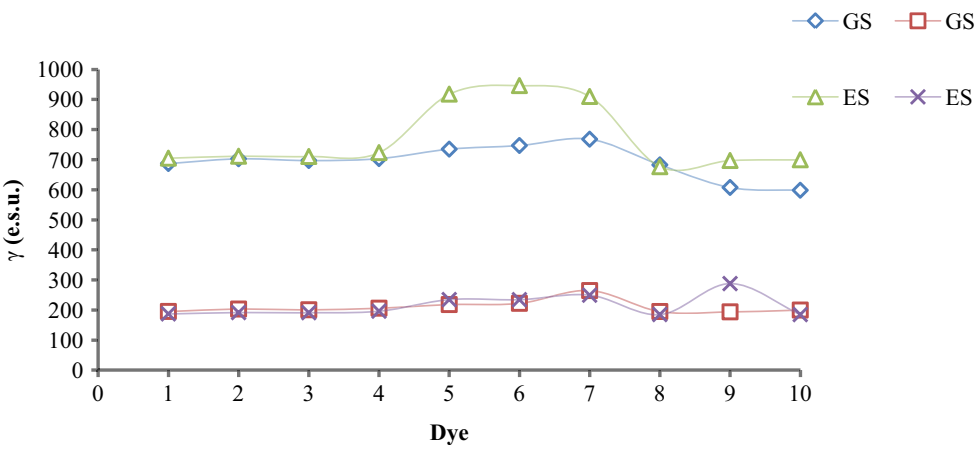

Fig. 7 Calculated values for second hyperpolarazibility γ (in esu) of dyes 1–10 in the ground state (GS) and the excited state (ES) in acetonitrile solvent and gas phase at the B3LYP/6-31G(d) Level

p-nitroaniline, while lowest static first hyperpolarazibilty value (β_o) observed for coumarin **9** which is 15 times greater than corresponding values of urea, and it is slightly more than that of p-nitroaniline in gas phase. The calculated value of p-nitroaniline in acetonitrile solvent is 13.6×10^{-30} esu [41]. But in acetonitrile solvent coumarin **8** shows 35.85×10^{-30} esu. It shows almost three times higher β_o value than the corresponding value of p-nitroaniline. From the Tables 4 and 5 we can see that β_o value of coumarin **8** is nearly 173 times greater than the corresponding values of urea, and 12 times higher than that of p-nitroaniline, while the lowest β_o value observed for coumarin **10** as compared to the other coumarins is 26 times greater than the corresponding values of urea, and two times higher than that of p-nitro aniline in acetonitrile solvent. This is because the ortho hydroxyl group of the rigid coumarin core makes intramolecular hydrogen bonding with nitrogen and makes the structure planar. Due to the planarity the intramolecular charge transfer (ICT) properties of the coumarin dyes get enhanced and result into an increase in β_o value. From these results, we can say that intramolecular charge transfer would be better facilitated by attachment of an electron-withdrawing substituent at the 3-position as well as planarity and rigidity of the chromophore. Because the first excited state in nonlinear optical chromophores typically exhibits intramolecular charge transfer in the same direction. We can conclude that the coumarin derivatives have considerable nonlinear optical properties. Figure 7 reveals that second hyperpolarizability is much higher in the excited state in acetonitrile solvent as compared to in the ground state. But such change is not observed in case of gas phase calculation. Coumarin **5**, **6** and **7** show higher γ values in the excited state as compared to the ground state. The Fig. 8 reveals that the mean first hyperpolarizability for coumarin **1**–**6** in acetonitrile solvent is higher in the ground state as compared to the excited state but for coumarin **7**–**9** it is less in the ground as compared to the excited state. However, in gas phase coumarin **1**–**6** show higher values as compared to the excited state but coumarin **7** and **9** show lower value in the gas phase. This anomalous behaviour of these coumarin dyes was observed due to the solubility factor and other structural parameters like hydroxy group and triphenyl amine group.

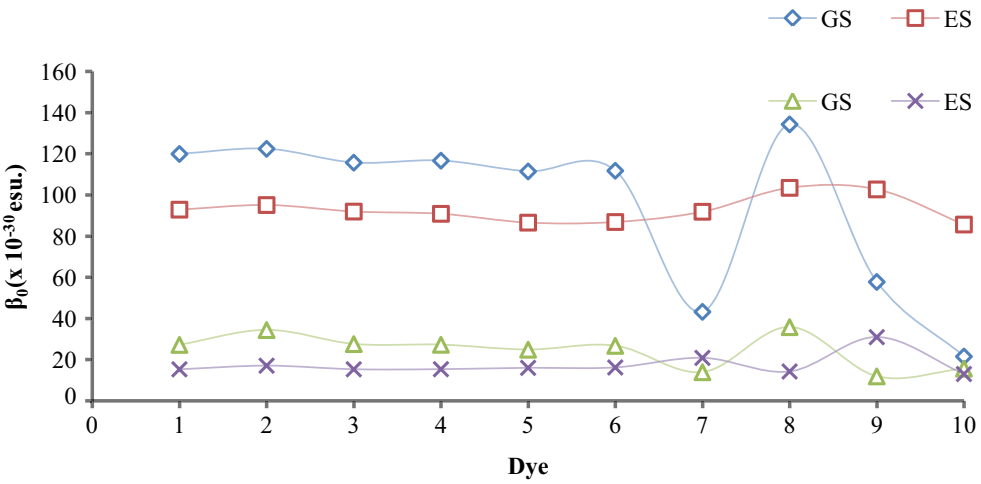

Fig. 8 Calculated values for mean first hyperpolarazibility β_0 (in esu) of dyes 1–10 in the ground state (GS) and the excited state (ES) in acetonitrile solvent and gas phase at the B3LYP/6-31G(d) Level

Conclusions

In this paper, we have studied structural properties and electronic spectral behaviour of rigid coumarin dyes in gas phase and acetonitrile solvent medium. DFT studies showed that there is a large increase in the dipole moment of the first excited state suggesting a pronounced change delocalization in the first excited state. The optimized geometries obtained from B3LYP/6-31G(d) and TD-B3LYP/6-31G(d) were examined by comparing the ground and excited state geometries and charge distribution. Vertical excitations and emissions were computed and compared with the experimental values. These dyes have shown a prominent absorption at the longer wavelength due to HOMO→LUMO transition with high oscillator strength and a small oscillator strength absorption band due to HOMO-1→LUMO for coumarin dyes **3** and **10**. The computed absorption and emission wavelengths are in good agreement with the experimental results. The first hyperpolarizability and static second order hyperpolarazibility were calculated using finite field approach and it was found that these dyes possess a large second-order nonlinear optical property and this is mainly due to the strong donor-π-acceptor conjugation due to rigid molecular system than simple coumarin molecule. These coumarin dyes shows the first order hyperpolarizability is 32–96 times greater than urea in gas phase and 58–363 times greater in acetonitrile medium. In summary, the reported results illustrate the ability of density functional theory calculations to determine and analyze the relationships between the structure and the NLO properties of organic dyes, in complement to experimental characterizations.

Acknowledgments Sandip K. Lanke is thankful to University Grant Commission (UGC) for providing junior and senior research fellowship.

References

1. Syzova ZA, Doroshenko AO, Lukatskaya LL et al (2004) Bichromophoric fluorescent dyes with rigid molecular structure: fluorescence ability regulation by the photoinduced intramolecular electron transfer. J Photochem Photobiol A Chem 165:59–68
2. Turki H, Abid S, Fery-Forgues S, El Gharbi R (2007) Optical properties of new fluorescent iminocoumarins: Part 1. Dye Pigment 73: 311–316
3. Christie RM, Lui C (2000) Studies of fluorescent dyes: part 2. An investigation of the synthesis and electronic spectral properties of substituted 3-(2′-benzimidazolyl)coumarins. Dye Pigment 47:79–89
4. Schill H, Nizamov S, Bottanelli F et al (2013) 4-Trifluoromethyl-substituted coumarins with large Stokes shifts: synthesis, bioconjugates, and their use in super-resolution fluorescence microscopy. Chemistry 19:16556–16565
5. Wagner BD (2009) The use of coumarins as environmentally-sensitive fluorescent probes of heterogeneous inclusion systems. Molecules 14:210–237
6. Bolte S, Talbot C, Boutte Y et al (2004) FM-dyes as experimental probes for dissecting vesicle trafficking in living plant cells. J Microsc 214:159–173
7. Yuan L, Lin W, Song J, Yang Y (2011) Development of an ICT-based ratiometric fluorescent hypochlorite probe suitable for living cell imaging. Chem Commun (Camb) 47:12691–12693
8. Cho S, Jang J, Song C et al (2013) Simple super-resolution live-cell imaging based on diffusion-assisted Förster resonance energy transfer. Sci Rep 3:1208
9. Signore G, Nifosì R, Albertazzi L et al (2010) Polarity-sensitive coumarins tailored to live cell imaging. J Am Chem Soc 132: 1276–1288
10. Peng M-J, Guo Y, Yang X-F et al (2013) A highly selective ratiometric and colorimetric chemosensor for cyanide detection. Dye Pigment 98:327–332
11. Tsukamoto K, Shinohara Y, Iwasaki S, Maeda H (2011) A coumarin-based fluorescent probe for Hg2+ and Ag+ with an N'-acetylthioureido group as a fluorescence switch. Chem Commun (Camb) 47:5073–5075
12. Li J, Zhang C-F, Yang S-H et al (2014) A coumarin-based fluorescent probe for selective and sensitive detection of thiophenols and its application. Anal Chem 86:3037–3042
13. Jones G, Jackson WR, Choi CY, Bergmark WR (1985) Solvent effects on emission yield and lifetime for coumarin laser dyes. Requirements for a rotatory decay mechanism. J Phys Chem 89: 294–300
14. Maeda M (1984) Laser Dyes. Academic, New York
15. Wang Z-S, Cui Y, Hara K et al (2007) A high-light-harvesting-efficiency coumarin dye for stable dye-sensitized solar cells. Adv Mater 19:1138–1141
16. Hara K, Sato T, Katoh R et al (2003) Molecular design of coumarin dyes for efficient dye-sensitized solar cells. J Phys Chem B 107: 597–606
17. Zhang R, Zheng H, Shen J (1999) A new coumarin derivative used as emitting layer in organic light-emitting diodes. Synth Met 106: 157–160
18. Chen CH, Tang CW (2001) Efficient green organic light-emitting diodes with stericly hindered coumarin dopants. Appl Phys Lett 79: 3711–3713
19. Jung HS, Ko KC, Lee JH et al (2010) Rationally designed fluorescence turn-on sensors: a new design strategy based on orbital control. Inorg Chem 49:8552–8557
20. Liu B, Wang R, Mi W et al (2012) Novel branched coumarin dyes for dye-sensitized solar cells: significant improvement in photovoltaic performance by simple structure modification. J Mater Chem 22:15379–15387
21. Yu T, Zhao M, Li A et al (2012) Synthesis and photoluminescent properties of 7-N, N-diphenylamino-3- benzoheterocyclic coumarin derivatives. Res Chem Intermed 39:2259–2266
22. Jagtap AR, Satam VS, Rajule RN, Kanetkar VR (2009) The synthesis and characterization of novel coumarin dyes derived from 1, 4-diethyl-1,2,3,4-tetrahydro-7-hydroxyquinoxalin-6-carboxaldehyde. Dye Pigment 82:84–89
23. Laurent AD, Adamo C, Jacquemin D (2014) Dye chemistry with time-dependent density functional theory. Phys Chem Chem Phys 16:14334–14356
24. Laurent AD, Jacquemin D (2013) TD-DFT benchmarks: A review. Int J Quantum Chem 113:2019–2039
25. Cramer CJ, Truhlar DG (2009) Density functional theory for transition metals and transition metal chemistry. Phys Chem Chem Phys 11:10757–10816
26. Furche F, Rappaport D (2005) Density functional theory for excited states: Equilibrium structure and electronic spectra. In: Olivucci M (ed) Comput Photochem. Elsevier, Amsterdam, pp 93–128
27. Oprea C, Panait P, Cimpoesu F et al (2013) Density functional theory (DFT) study of coumarin-based dyes adsorbed on TiO2

nanoclusters—applications to dye-sensitized solar cells. Mater (Basel) 6:2372–2392
28. Bai Y, Du J, Weng X (2014) Synthesis, characterization, optical properties and theoretical calculations of 6-fluoro coumarin. Spectrochim Acta A Mol Biomol Spectrosc 126:14–20
29. Frisch MJ, Trucks GW, Schlegel HB et al (2009) Gaussian 09, Revision C.01. Gaussian 09, Revis B01. Gaussian, Inc, Wallingford
30. Treutler O, Ahlrichs R (1995) Efficient molecular numerical integration schemes. J Chem Phys 102:346–354
31. Becke AD (1993) Density-functional thermochemistry. III. The role of exact exchange. J Chem Phys 98
32. Lee C, Yang W, Parr RG (1988) Development of the Colle-Salvetti correlation-energy formula into a functional of the electron density. Phys Rev B 37:785–789
33. Hehre WJ, Radom L, Schleyer PV, Pople J (1986) Ab Initio Molecular Orbital Theory. Wiley, New York
34. Bauernschmitt R, Ahlrichs R (1996) Treatment of electronic excitations within the adiabatic approximation of time dependent density functional theory. Chem Phys Lett 256:454–464
35. Valeur B, Berberan-Santos MN (2001) Molecular fluorescence: principles and applications. Wiley, Weinheim
36. Tomasi J, Mennucci B, Cammi R (2005) Quantum mechanical continuum solvation models. Chem Rev 105:2999–3094
37. Cossi M, Barone V, Cammi R, Tomasi J (1996) Ab initio study of solvated molecules: a new implementation of the polarizable continuum model. Chem Phys Lett 255:327–335
38. Ditchfield R, Hehre WJ, Pople JA (1971) Self-consistent molecular-orbital methods. IX. An extended gaussian-type basis for molecular-orbital studies of organic molecules. J Chem Phys 54: 724–728
39. Hehre WJ, Ditchfield R, Pople JA (1972) Self—consistent molecular orbital methods. XII. further extensions of gaussian—type basis sets for use in molecular orbital studies of organic molecules. J Chem Phys 56:2257–2261
40. Kleinman DA (1962) Nonlinear dielectric polarization in optical media. Phys Rev 126:1977–1979
41. Stähelin M, Burland DM, Rice JE (1992) Solvent dependence of the second order hyperpolarizability in p-nitroaniline. Chem Phys Lett 191:245–250